Magnetic Ordering in Materials with Singlet Crystal-Field Ground State. II. Behavior in the Ordered State or in an Applied Field

YUNG-LI WANG
University of Pittsburgh, Pittsburgh, Pennsylvania 15213*
and
Florida State University,† Tallahassee, Florida 32306

AND

BERNARD R. COOPER
General Electric Research and Development Center, Schenectady, New York 12301

(Received 20 March 1969)

The theory of magnetic ordering and of collective excitation behavior in materials with a singlet crystal-field ground state has been extended to finite temperature and to the regime where the system has a magnetic moment due to ordering or an applied field. For simplicity, we still consider a system where the only excited state in the absence of exchange is also a singlet at an energy Δ (in units of °K) above the ground state. We show that in the random-phase approximation (RPA), the self-consistent molecular-field eigenstates serve as a good basis for determining the collective excitation energies; while in the two-site correlation approximation (TSCA), a modification of the molecular-field states is required in the ordered phase. The energies of the collective excitations are calculated with and without an external magnetic field in both the paramagnetic and magnetically ordered phases. At finite temperatures, a Green's-function formalism is employed to facilitate the calculation of thermodynamic quantities. For $T_C/\Delta \geq 0.1$, we find in the RPA a discontinuity in the magnetization at the critical point. The discontinuity is most prominent when T_C is comparable to the crystal-field splitting Δ, and vanishes both as T_C/Δ decreases toward 0.1 and at $\Delta=0$. We show that in the TSCA the magnetic transition is also first order, and, in fact, for the TSCA the transition is first order even at $T=0$. The specific heat and susceptibility are calculated in both the RPA and the TSCA and compared with the molecular-field-theory results.

1. INTRODUCTION

FOR rare-earth compounds with a singlet crystal-field ground state for the rare-earth ion, the exchange interaction must exceed a certain critical value relative to the crystal field to have magnetic ordering even at zero temperature.[1–4] The magnetic moment which occurs in such a case is essentially an induced moment corresponding to the Van Vleck susceptibility, where the exchange field takes the place of an applied external magnetic field.

In a previous paper[5] (referred to as I hereafter), we discussed the collective excitation behavior and the magnetic ordering in systems with singlet crystal-field ground state. In particular, we studied the energies of collective excitations for the two-level system where the first excited state is also a singlet. We showed that a general and useful way to treat the collective excitation behavior in induced moment systems is through the introduction of a pseudospin formalism, where the expectation value of S_{iz}, the pseudospin for the ith ion, corresponds to the occupation of the molecular-field states for that ion. (The expectation value of S_{iz} for the true ground state would be $-\frac{1}{2}$ if the molecular-field approximation were exact.) Such a formulation lends itself to the use of techniques developed for conventional spin systems in order to obtain a succession of approximations treating correlation effects more correctly.

In I, we found the collective excitation behavior for the two-singlet-state system in the paramagnetic regime in the absence of applied magnetic field. While the formal treatment was presented for general temperature, the self-consistent numerical calculations presented were restricted to zero temperature.

In the present paper, we have extended the treatment of the collective excitation behavior to the regime, where the system has a net magnetic moment either through the presence of magnetic ordering or through the presence of an applied magnetic field in the paramagnetic regime. In general, doing this involves certain formal difficulties connected with finding an appropriate basis for treating collective excitations corresponding to small perturbations from the states of the basis. In Sec. 2, we examine these questions in some detail before specializing to the random-phase approximation (RPA) and the two-site correlation approximation (TSCA).

For the RPA, it has been possible to carry out self-consistent detailed numerical calculations of the collective excitation spectrum and of the corresponding magnetization in the ordered regime. Also, we have extended the numerical calculations in the paramagnetic regime to finite temperatures. This has allowed us to follow the collective excitation and magnetization behavior through the ordering temperature, and also to study the change in the type of behavior found as the exchange

* Supported by U. S. Air Force Office of Scientific Research.
† Present address.
[1] G. T. Trammell, J. Appl. Phys. **31**, 362S (1960).
[2] G. T. Trammell, Phys. Rev. **131**, 932 (1963).
[3] B. Bleaney, Proc. Roy. Soc. (London) **276A**, 19 (1963).
[4] B. R. Cooper, Phys. Rev. **163**, 444 (1967).
[5] Y.-L. Wang and B. R. Cooper, Phys. Rev. **172**, 539 (1968). (Referred to as I throughout the present paper.)

increases so that the ratio of Curie temperature to crystal-field splitting (T_c/Δ) increases. (In this paper we will use Boltzmann's constant as the unit of energy, i.e., all energies are in °K.) In the RPA, at $T=0$ the magnetic transition is second order, and there is a $\mathbf{k}=0$ mode instability at the critical ratio of exchange to crystal-field splitting for magnetic ordering. For $T_C/\Delta \geq 0.1$, the transition becomes first order, although for values of T_C/Δ only slightly greater than 0.1, the discontinuity in magnetization at T_C is small. The discontinuity is most significant for values of T_C/Δ near unity, where it is quite substantial. For $T_C/\Delta \gg 1$, while a discontinuity in magnetization persists, the size of discontinuity decreases, and the magnetization approaches the molecular-field behavior.[6] (This approach to molecular-field behavior, as discussed in Sec. 6 below, is associated with the fact that the collective excitations we treat do not approach spin waves for large exchange, but rather the excitation dispersion disappears, and one approaches a molecular-field-type excited state.)

For the TSCA, we have treated the detailed self-consistent calculations only in the limit where the Curie temperature is high compared to the crystal-field splitting ($T_C/\Delta \gg 1$). However, we are able to use our understanding of that limiting behavior to show that the discontinuity of magnetic moment at the critical point occurs for all finite T_C/Δ in the TSCA. In fact, contrary to our assumption in I, we are able to show for the TSCA that the transition is first order even at $T=0$.

It has been possible to calculate the susceptibility for the TSCA in the paramagnetic temperature regime, and this differs significantly from the RPA susceptibility values in the critical region.

We have also calculated the specific heat for the molecular-field approximation, the RPA and the TSCA in the paramagnetic regime, and for the molecular-field approximation and the RPA (for small T_C/Δ) in the ferromagnetic regime. Because of the presence of the dispersion in collective excitations, the Schottky anomaly in the paramagnetic regime is appreciably broadened in the RPA and the TSCA. (In the molecular-field approximation, the exchange has no effect on the specific heat in the paramagnetic regime.)

In Sec. 2, we present the general formalism of the pseudospin treatment for the two-singlet-level system with a magnetic moment. This formalism is treated in the RPA in Sec. 3, and formal expressions are obtained for excitation energies, spontaneous magnetization, and susceptibility. The formalism is treated in the TSCA in Sec. 4 and the treatment is specialized to the limit of small moment to obtain the paramagnetic susceptibility. In Sec. 5, we calculate the specific heat. Finally, in Sec. 6 we present the results of the numerical calculations, and discuss the physical effects giving rise to the behavior found. We also mention the experimental situation most likely to provide information related to the present model behavior.

2. PSEUDOSPIN FORMALISM WHEN A TWO-LEVEL SYSTEM HAS MAGNETIC MOMENT

We consider the Hamiltonian

$$\mathcal{H}=\sum_i (V_{ci}-g\mu_B H J_{iz})-\sum_{\langle i,j\rangle} \mathcal{J}_{ij}\mathbf{J}_i\cdot\mathbf{J}_j. \tag{2.1}$$

Here, V_{ci} is the single-ion crystal-field potential, which gives a singlet ground state and a singlet excited state separated by an energy gap Δ. In (2.1), $\mathbf{J}_i$ is the total angular momentum of the rare-earth ion at the ith site, and $\mathcal{J}_{ij}$ represents the effective exchange integral. [In real systems with large orbital contribution to the moment, there may also be a substantial anisotropic exchange[7,8] of the form $\sim(\mathbf{J}_i\cdot\mathbf{R}_{ij})(\mathbf{J}_j\cdot\mathbf{R}_{ij})$. Such a contribution could also be treated by the present formalism.] The sum in the exchange term is over all interacting pairs of ions. We have included a Zeeman term in the Hamiltonian, where g and μ_B denote the g factor and Bohr magneton. (As already stated, we use Boltzmann's constant as the unit of energy, so Δ/T, $\mathcal{J}/\Delta$, and $g\mu_B H/T$ are pure numbers. In these units, for H in oersteds, $\mu_B=0.6717\times10^{-4}$ °K/Oe.)

We can split the total Hamiltonian into two parts as

$$\mathcal{H}=\mathcal{H}_0+\mathcal{H}_1, \tag{2.2}$$

where

$$\mathcal{H}_0=\sum_i \{V_{ci}-[g\mu_B H+2\mathcal{J}(0)\langle J\rangle]J_{iz}\}+N\mathcal{J}(0)\langle J\rangle^2 \tag{2.3}$$

and

$$\mathcal{H}_1=-\sum_{\langle i,j\rangle}\mathcal{J}_{ij}\mathbf{j}_i\cdot\mathbf{j}_j. \tag{2.4}$$

Here we have defined

$$\mathbf{j}_i\equiv\mathbf{J}_i-\langle J\rangle\hat{\epsilon}_z, \tag{2.5}$$

and

$$\mathcal{J}(k)\equiv\sum_j \mathcal{J}_{ij}e^{i\mathbf{k}\cdot\mathbf{r}_{ij}}. \tag{2.6}$$

Then $\mathcal{H}_0$ is the molecular-field Hamiltonian. In (2.5), $\hat{\epsilon}_z$ denotes a unit vector in the z direction. The quantity $\langle J\rangle$ is the statistical average of the angular momentum per ion J_{iz} and must be determined self-consistently. At zero temperature and in the molecular-field approxima-

[6] A paper by Pink treating this problem in an approximation essentially equivalent to our RPA appeared while the present manuscript was in preparation. [D. A. Pink, J. Phys. C1, 1246 (1968).] Pink has found a similar discontinuity in magnetization at T_c. However, Pink makes the statement that the magnetization is discontinuous at all finite T_c. In contrast, we find that there is a discontinuity only for $T_c/\Delta \geq 0.1$. For $T_c/\Delta < 0.1$, the transition is second order. Presumably, Pink's incorrect statement was simply an erroneous assumption which was not investigated fully, and his formal development and detailed calculations as far as they go appear to be correct.

[7] R. J. Elliott and M. F. Thorpe, J. Appl. Phys. **39**, 802 (1968).
[8] P. M. Levy, Phys. Rev. **135**, A155 (1964); **147**, 311 (1966).

tion, $\langle J\rangle$ is the expectation value of J_{iz} over the molecular-field ground state.

To obtain the molecular-field eigenstates, we diagonalize $\mathcal{H}_0$. These molecular-field eigenstates are

$$|0\rangle=\cos\theta|0_c\rangle+\sin\theta|1_c\rangle, \tag{2.7a}$$

$$|1\rangle=-\sin\theta|0_c\rangle+\cos\theta|1_c\rangle. \tag{2.7b}$$

Here, $|0_c\rangle$ and $|1_c\rangle$ are the crystal-field ground and excited state, respectively, which can be obtained by solving the crystal-field Hamiltonian V_c. In our general discussion we do not need the explicit form of the two states which may differ from material to material. We only assume that they are magnetic singlets.

The rotation angle which diagonalizes $\mathcal{H}_0$ is given by

$$\tan2\theta=2[2\mathcal{J}(0)\langle J\rangle+g\mu_BH]\alpha/\Delta, \tag{2.8}$$

where

$$\alpha\equiv\langle1_c|J_z|0_c\rangle \tag{2.9}$$

is the off-diagnonal matrix element of the angular momentum between the crystal-field-only states. As already stated, Δ is the energy gap between the two crystal-field-only singlets.

As discussed in I, the pseudospin representation for the Hamiltonian of (2.1) is based on the fact that the matrix elements for a two-level system can always be written in terms of an effective spin Hamiltonian with spin equal to $\frac{1}{2}$. We assign $S_z=-\frac{1}{2}$ to the molecular-field ground state, and $S_z=\frac{1}{2}$ to the molecular-field excited state. Then to project $\mathcal{H}$ onto the pseudospin manifold only involves recognizing the form of the four spin-$\frac{1}{2}$ operators, which correspond to 2×2 matrices with unity as one element, and zero as the other three elements. These operators are S_i^+, S_i^-, $S_i^-S_i^+$, and $S_i^+S_i^-$.

In I, we made the specialization pertinent to the paramagnetic regime in the absence of applied field, namely, that $\langle J\rangle=0$, $\theta=0$. We now proceed to treat the case when the system has a magnetic moment, so $\theta\neq0$. From Eq. (3.1) of I we obtain

$$\mathcal{H}=\sum_i C_zS_{iz}+2\sum_i C_xS_{ix}+\sum_{\langle i,j\rangle}\mathcal{J}_{ij}(C_{zz}S_{iz}S_{jz}+4C_{xx}S_{ix}S_{jx}+4C_{xz}S_{ix}S_{jz}), \tag{2.10}$$

where, including the applied field, the energy splitting between the molecular-field states is

$$\epsilon_0=\Delta\cos2\theta+2[2\mathcal{J}(0)\langle J\rangle+g\mu_BH]\alpha\sin2\theta \tag{2.11}$$

and

$$C_z=[\epsilon_0-\mathcal{J}(0)(\alpha_{11}^2-\alpha_{00}^2)]=\Delta\cos2\theta+2g\mu_BH\alpha\sin2\theta, \tag{2.12a}$$

$$C_{zz}\equiv-(\alpha_{11}-\alpha_{00})^2=-4\alpha^2\sin^22\theta, \tag{2.12b}$$

$$C_{xx}\equiv-\alpha_{10}^2=-\alpha^2\cos^22\theta, \tag{2.12c}$$

$$C_x\equiv-\mathcal{J}(0)\alpha_{10}(\alpha_{00}+\alpha_{11})=2\mathcal{J}(0)\alpha\langle J\rangle\cos2\theta, \tag{2.12d}$$

$$C_{xz}\equiv-\alpha_{10}(\alpha_{11}-\alpha_{00})=2\alpha^2\sin2\theta\cos2\theta. \tag{2.12e}$$

When rewritten in this form, the fundamental difficulty associated with the calculations is apparent.

If we consider the equations of motion of the pseudospin operators S_i in order to find the excitation energies, e.g., at $T=0$, we are interested in small deviations from the equilibrium direction in pseudospin space. For the paramagnetic regime, the equilibrium direction in the pseudospin space is the z axis. In general, when the system has a moment ($\theta\neq0$) this is no longer true, and a further transformation of the type $S_{z'}=\beta S_z+\gamma S_x$ is required before one can calculate the elementary excitations, which show small deviations from the ground state with pseudospin pointing along the equilibrium direction. (We recall that physically the z axis in pseudospin space corresponds to the choice of the molecular-field states as the basis for representing the true states of the system. Transformation to an equilibrium direction in pseudospin space along a different axis corresponds to a different choice of basis for representing the true states of the system. Small deviations from the equilibrium direction of pseudospin correspond to small deviations of the true states of the system from the basis states used to define the pseudospin.) This difficulty arises because of the presence of the C_x and C_{xz} terms in $\mathcal{H}$. This is easily seen by considering the case when the z axis is the pseudospin equilibrium direction. Then so far as the ith pseudospin is concerned, there are three kinds of terms: The C_z term and the C_{zz} term (because S_{jz} has a nonvanishing time average) act like effective static fields longitudinal with respect to the assumed equilibrium direction. The C_{xx} term acts like a fluctuating field transverse with respect to the assumed equilibrium direction, since the time average of S_{jx} vanishes. The C_x term and the C_{xz} (because S_{jz} has a nonvanishing time average) act like static fields transverse to the assumed equilibrium direction. This means that unless the effect of the C_x and C_{xz} terms vanish, the assumed equilibrium direction is incorrect, and the equilibrium direction of the pseudospin changes so that there is no effective static transverse field.

Thus, in general we need a further coordinate transformation in the pseudospin space (from the axes determined by the use of the molecular-field states as basis for the pseudospin representation) before calculating the elementary excitation energies. However, if it happens that the C_x and C_{xz} terms cancel each other, we need no further coordinate transformation. In that case the basis we are using, which consists of the molecular-field-theory states, is a proper basis. (This is analogous to choosing the Néel state and the states having spin flips from the Néel state as the basis for studying spin waves in antiferromagnets.) We may, therefore, expect that in the RPA, which neglects the correlation of pseudospin motion on different lattice sites (so that for specified magnetization the effective field is the same as that in molecular-field theory), the cancellation of C_x and C_{xz} terms occurs, and one does

not have to make any pseudospin coordinate transformation. [This is in contrast to an improved approximation such as the TSCA, where the effective field and the consequent mixing of the crystal-field states is not simply given by the effects of magnetization plus applied field as shown in (2.8). The transformation to a proper basis for the TSCA takes account of the further mixing of the crystal-field states due to the effective field associated with correlation effects.] If one does need a transformation in a more exact treatment (such as the TSCA), the transformed Hamiltonian takes the same form as $\mathcal{H}$ in (2.10) with new coefficients.

It is easy to show that in terms of the pseudospin components J_z is given as

$$J_z=(-2\alpha\sin2\theta)S_z+(2\alpha\cos2\theta)S_x. \quad (2.13)$$

If a rotation of coordinates is necessary in order to eliminate the C_x and C_{xz} terms from the Hamiltonian, let us call the angle of rotation, in the x-z plane, of the z' axis from the z axis, φ. Then,

$$J_z=-2\alpha\sin(2\theta-\varphi)S_{z'}+2\alpha\cos(2\theta-\varphi)S_{x'}, \quad (2.14)$$

so that the self-consistent condition for the thermal average value of J_z is

$$\langle J\rangle=-2\alpha\langle S_{z'}\rangle\sin(2\theta-\varphi). \quad (2.15)$$

Bearing this in mind, we now consider in more detail the determination of the angle φ. As already stated above, this angle determines the transformation necessary in order to eliminate the effect of the C_x and C_{xz} terms and thus transform the Hamiltonian into the form appropriate for finding the elementary excitation energies. To do this, we write S_z in the form used by Callen[9] in treating ordinary spin systems:

$$S_z=\langle S_z\rangle+[(\tfrac{1}{2}-\langle S_z\rangle)S^+S^--(\tfrac{1}{2}+\langle S_z\rangle)S^-S^+]. \quad (2.16)$$

At $T=0$, $\langle S_z\rangle$ is the ground-state expectation value, while at finite temperature, $\langle S_z\rangle$ is the thermal average. Expression (2.16) is exact, and the quantity in brackets is small for all temperatures. Using (2.16), we rewrite $S_{ix}S_{jz}$ as

$$S_{ix}S_{jz}=\langle S_z\rangle S_{ix}+S_{ix}\times[(\tfrac{1}{2}-\langle S_z\rangle)S_j^+S_j^--(\tfrac{1}{2}+\langle S_z\rangle)S_j^-S_j^+]. \quad (2.17)$$

This allows us to combine the main part of the C_{xz} term in $\mathcal{H}$ with the C_x term. Substituting (2.17) into (2.10), we then consider the equation of motion of S_f^+:

$$\begin{aligned}[S_f^+,\mathcal{H}]=&-C_zS_f^++2[C_x+2\mathcal{J}(0)\langle S_z\rangle C_{xz}]S_{fz}\\&+2\sum_j\mathcal{J}_{fj}C_{xz}\{S_{fz}[(1-2\langle S_z\rangle)S_j^+S_j^-\\&-(1+2\langle S_z\rangle)S_j^-S_j^+]+(S_j^++S_j^-)\\&\times[(1-2\langle S_z\rangle)S_f^+S_{fz}-(1+2\langle S_z\rangle)S_{fz}S_f^+]\}\\&+\sum_j\mathcal{J}_{fj}[-2C_{zz}S_f^+S_{fz}+4C_{xx}S_{fz}(S_j^++S_j^-)]. \quad (2.18)\end{aligned}$$

[9] H. B. Callen, Phys. Rev. **130**, 890 (1963).

In this equation, the terms multiplying S_{fz} which have nonzero time averages correspond to static transverse fields. Then the condition that the terms acting like a transverse field sum to zero gives

$$0=\{2[C_x+2\mathcal{J}(0)\langle S_z\rangle C_{xz}]-8\sum_j\mathcal{J}_{fj}C_{xz}\langle S_z\rangle(\langle S_f^+S_j^+\rangle+\langle S_f^+S_j^-\rangle)\}S_{fz}, \quad (2.19)$$

where we have made the approximations

$$S_{fz}[(1-2\langle S_z\rangle)S_j^+S_j^--(1+2\langle S_z\rangle)S_j^-S_j^+]\approx0, \quad (2.20)$$

and

$$(S_j^++S_j^-)S_f^+S_{fz}\rightarrow(\langle S_j^+S_f^+\rangle+\langle S_j^-S_f^+\rangle)S_{fz}, \quad (2.21a)$$

$$(S_j^++S_j^-)S_{fz}S_f^+\rightarrow(\langle S_j^+S_f^+\rangle+\langle S_j^-S_f^+\rangle)S_{fz} \quad (2.21b)$$

considering only nearest-neighbor exchange interaction.

We can write (2.19) using the quantity ϵ defined in Eq. (4.10) of I

$$\epsilon=\frac{1}{N}\sum_k\gamma_k(\langle S_k^+S_k^-\rangle+\langle S_k^+S_{-k}^+\rangle)=\frac{1}{N}\sum_k\gamma_k(\langle S_k^+S_k^-\rangle+\langle S_k^-S_{-k}^-\rangle), \quad (2.22)$$

with

$$\gamma_k=\mathcal{J}(k)/\mathcal{J}(0) \quad (2.23)$$

so that (2.19) becomes

$$C_x+2C_{xz}\mathcal{J}(0)\langle S_z\rangle(1-2\epsilon)=0. \quad (2.24)$$

It should also be pointed out that the particular form of the equation determining φ depends on the way in which we write S_z. We have chosen to write S_z in Callen's form, so that the approximations made always involve small quantities.

Thus, to satisfy Eq. (2.24), we have to transform to the x', y', and z' coordinates such that

$$S_z'=S_z\cos\varphi+S_x\sin\varphi, \quad (2.25a)$$

$$S_x'=-S_z\sin\varphi+S_x\cos\varphi, \quad (2.25b)$$

$$S_y'=S_y. \quad (2.25c)$$

After the rotation, the Hamiltonian takes the same form as in (2.10), but with different coefficients:

$$C_z'=\Delta\cos(2\theta-\varphi)+2g\mu_B\alpha H\sin(2\theta-\varphi), \quad (2.26a)$$

$$C_{z'z'}=-4\alpha^2\sin^2(2\theta-\varphi), \quad (2.26b)$$

$$C_{x'x'}=-\alpha^2\cos^2(2\theta-\varphi), \quad (2.26c)$$

$$C_{x'}=\tfrac{1}{2}\Delta\sin(2\theta-\varphi)-g\mu_B\alpha H\cos(2\theta-\varphi), \quad (2.26d)$$

$$C_{x'z'}=\alpha^2\sin^2(2\theta-\varphi). \quad (2.26e)$$

Then substitution of (2.26d) and (2.26e) into (2.24) [with $x\rightarrow x'$, $z\rightarrow z'$ in (2.24)] gives the equation deter-

mining φ. Namely,

$$\tfrac{1}{2}\Delta \sin(2\theta-\varphi)+4\mathcal{J}(0)\alpha^2\langle S_z\rangle(1-2\epsilon)\sin(2\theta-\varphi)\times\cos(2\theta-\varphi)-g\mu_B\alpha H\cos(2\theta-\varphi)=0\,. \quad (2.27)$$

In the absence of external magnetic field, $H=0$, and we have either $\varphi=2\theta$ or

$$\cos(2\theta-\varphi)=\Delta/-8\langle S_z\rangle\mathcal{J}(0)\alpha^2(1-2\epsilon)\,. \quad (2.28)$$

[Actually, $\varphi=2\theta$ is the solution of $C_x=0$, $C_{xz}=0$, and is independent of the approximations used in Eqs. (2.20) and (2.21). What this solution does is to undo the transformation given in (2.7) and (2.8) and bring us back to the crystal-field-only eigenstate basis, which is, of course, far from the proper basis for which we are looking. However, putting aside the demand of choosing the proper basis for the perturbation considerations, any complete set of wave functions is eligible for a basis. In the special representation using the crystal-field-only eigenstates as basis the Hamiltonian takes the simplest form

$$\mathcal{H}=\sum_i \Delta S_{iz}-4\sum_{\langle i,j\rangle}\mathcal{J}_{ij}\alpha^2 S_{ix}S_{jx}, \quad (2.29)$$

which is, in fact, Eq. (3.8) of I. However, here in the ordered phase $\langle S_x\rangle=0$. As we have pointed out in I, Eq. (2.34) is identical to that for an Ising spin system with a transverse magnetic field, and may serve as a good starting point for an exact calculation.]

For the purpose of calculating the elementary excitation energies in the ordered regime, we use Eq. (2.28) to determine the value of φ eliminating the effective transverse field.

In the RPA as discussed in I, we take $\langle S_j^+S_f^+\rangle=\langle S_j^-S_f^+\rangle=0$, so that $\epsilon=0$. Then in the RPA, the condition for the vanishing of transverse field effects in the equations of motion becomes

$$\text{RPA,}\quad C_x+2\mathcal{J}(0)C_{xz}\langle S_z\rangle=0. \quad (2.30)$$

In agreement with our earlier remarks concerning the absence of any rotation of pseudospin coordinates in the RPA, we see that this condition is automatically satisfied with $\varphi=0$, if we remember that both C_x and C_{xz} are functions of $\langle J\rangle$, which should be evaluated self-consistently. From (2.15),

$$\text{if } \varphi=0,\quad \langle J\rangle=-2\alpha\langle S_z\rangle\sin2\theta, \quad (2.31)$$

and from (2.12d) and (2.12e)

$$C_x+2\mathcal{J}(0)C_{xz}\langle S_z\rangle=2\alpha\mathcal{J}(0)\cos2\theta(\langle J\rangle+2\alpha\sin2\theta\langle S_z\rangle). \quad (2.32)$$

So that, indeed, (2.30) is satisfied for $\varphi=0$.

In Sec. 3, using the basic simplification that $\varphi=0$, we consider the collective excitation and magnetization behavior in the RPA. In Sec. 4, we treat the more complicated case of the TSCA, where $\varphi\neq0$.

3. RPA THEORY FOR A TWO-LEVEL SYSTEM WITH NET MAGNETIC MOMENT

We now treat the two-singlet-level system in the RPA, when each ion has a net moment. This applies either when the system is magnetically ordered, or when there is an applied magnetic field present in the paramagnetic regime. We first consider the situation at $T=0$ using the equations of motion for the pseudospin operators. The results are then extended to finite temperature by studying the equations of motion for the retarded time Green's functions.

A. Behavior at $T=0$

The Fourier transformed equations of motion for the pseudospin in the RPA are

$$i\dot{S}_k^+=[S_k^+,\mathcal{H}]=-C_zS_k^+-2C_{zz}\langle S_z\rangle\mathcal{J}(0)S_k^+ +4C_{xx}\langle S_z\rangle\mathcal{J}(k)(S_k^++S_{-k}^-) =-\beta S_k^++\lambda S_{-k}^-, \quad (3.1a)$$

$$i\dot{S}_{-k}^-=[S_{-k}^-,\mathcal{H}]=C_zS_{-k}^-+2C_{zz}\langle S_z\rangle\mathcal{J}(0)S_{-k}^- -4C_{xx}\langle S_z\rangle\mathcal{J}(k)(S_k^++S_{-k}^-) =\beta S_{-k}^--\lambda S_k^+, \quad (3.1b)$$

where condition (2.30) has been used, and

$$S_k^+=\frac{1}{N}\sum_g S_g^+e^{-i\mathbf{k}\cdot\mathbf{r}_g}, \quad (3.2)$$

$$\beta=C_z+2C_{zz}\langle S_z\rangle\mathcal{J}(0)-4C_{xx}\langle S_z\rangle\mathcal{J}(k)\,, \quad (3.3)$$

$$\lambda=4C_{xx}\langle S_z\rangle\mathcal{J}(k)\,. \quad (3.4)$$

Thus, the normal mode energies are given by

$$E_k^2=\beta^2-\lambda^2=[C_z+2C_{zz}\langle S_z\rangle\mathcal{J}(0)]\times[C_z+2C_{zz}\langle S_z\rangle\mathcal{J}(0)-8C_{xx}\langle S_z\rangle\mathcal{J}(k)]. \quad (3.5)$$

We now consider separately the cases of the ordered phase with $H=0$, the paramagnetic phase with finite H, and the ordered phase with finite H.

a. $H=0$, Ordered Phase

To evaluate the coefficients in (3.5), we use (2.8) with $H=0$ and (2.31) to get

$$\cos2\theta=-1/(2\langle S_z\rangle A)\,, \quad (3.6)$$

with

$$A=4\mathcal{J}(0)\alpha^2/\Delta \quad (3.7)$$

defined as in I. Then,

$$E_k/\Delta=(1/a)(1-a^2\gamma_k)^{1/2}\,, \quad (3.8)$$

where

$$a=-1/(2\langle S_z\rangle A)\,. \quad (3.9)$$

The spectrum of (3.8) differs from the boson spectrum obtained in the Bogoliubov-type approximation[10] by having replaced $-\frac{1}{2}$ by $\langle S_z\rangle$ as expected.

[10] B. Grover, Phys. Rev. **140**, A1944 (1965).

b. $H\neq 0$, Paramagnetic Phase

First, we consider the limit of small H, since that is the pertinent limit for calculating the susceptibility. As $H\to 0$, $\langle J\rangle\to 0$, and therefore $\theta\to 0$. Then in the limit of small H, we can replace $\sin 2\theta$ in (2.31) by the expression for $\tan 2\theta$ in (2.8) and obtain

$$H\to 0,\quad \langle J\rangle=-2\langle S_z\rangle(A\langle J\rangle+2\alpha^2 g\mu_B H/\Delta) \tag{3.10}$$

or

$$\langle J\rangle=(2\alpha^2 g\mu_B/\Delta)[-2\langle S_z\rangle H/(1+2\langle S_z\rangle A)]. \tag{3.11}$$

So that the susceptibility is

$$T=0,\ \chi=(2\alpha^2 g^2\mu_B{}^2 k_B/\Delta)[-2\langle S_z\rangle/(1+2\langle S_z\rangle A)]. \tag{3.12}$$

Here $\langle S_z\rangle$ denotes the expectation value for the true ground state.

We next obtain the excitation spectrum in the paramagnetic regime in an applied field at $T=0$, and show the connection with the Bogoliubov-type spectrum obtained by Cooper,[4] including terms up to second order in H. Defining

$$B=2\alpha^2 g\mu_B/\Delta \tag{3.13}$$

and evaluating the coefficients to second order in H, we obtain the energy spectrum

$$\frac{E_k}{\Delta}=\left[1-\frac{\gamma_k}{a}+\frac{B^2H^2}{\alpha^2(1-1/a)^2}\left(1+\frac{\gamma_k}{2a}\right)\right]^{1/2} \tag{3.14}$$

with a as defined in (3.9). This would coincide with Cooper's result if $-2\langle S_z\rangle=1$.

c. Spectrum for Ordered Phase with $H\neq 0$

We define

$$h=2\alpha g\mu_B H/\Delta. \tag{3.15}$$

For small h, i.e., $h\ll 1/a^2-1$,

$$E_k=(\Delta/a)[1-a^2\gamma_k+2h(1/a^2-1)^{-1/2}(1+\tfrac{1}{2}a^2\gamma_k)]^{1/2}. \tag{3.16}$$

This is the behavior for exchange well above the critical value for the $\mathbf{k}=0$ mode instability.

On the other hand, for $1\gg h\gg(1/a^2-1)$, we have

$$E_k=\Delta[1-\gamma_k+\tfrac{1}{2}(2h)^{2/3}(1+2\gamma_k)]^{1/2}, \tag{3.17}$$

so that the energy gap is still finite at $a=1$.

B. Behavior at Finite Temperature

The calculations are extended to finite temperature by using the retarded time Green's-function formalism.[11] Here, we briefly summarize the procedure, since the calculation parallels that already done in Sec. 3 A for $T=0$. Following the procedure of I (used there for the paramagnetic regime in the absence of applied field), we define two types of Green's functions:

$$G^-(g,l)=-i\langle[S_g{}^-(t),S_l{}^+(0)]\rangle\theta(t)=\langle\langle S_g{}^-(t);S_l{}^+(0)\rangle\rangle, \tag{3.18}$$

$$G^+(g,l)=-i\langle[S_g{}^+(t),S_l{}^+(0)]\rangle\theta(t)=\langle\langle S_g{}^+(t);S_l{}^+(0)\rangle\rangle. \tag{3.19}$$

Here, $\theta(t)$ is the usual unit step function, and the canonical thermal average is indicated by the single angular brackets. The equations of motion of the Green's functions in the energy Fourier space are

$$EG_E{}^-(g,l)=-\frac{1}{\pi}\langle S_z\rangle\delta_{gl}+[C_z+2C_{zz}\langle S_z\rangle\mathcal{J}(0)]G_E{}^-(g,l)-4C_{xx}\langle S_z\rangle\sum_f \mathcal{J}_{fg}[G_E{}^-(f,l)+G_E{}^+(f,l)]-2[C_x+2C_{xz}\langle S_z\rangle\mathcal{J}(0)]G_E{}^z(g,l), \tag{3.20}$$

$$EG_E{}^+(g,l)=-[C_z+2C_{zz}\langle S_z\rangle\mathcal{J}(0)]G_E{}^+(g,l)+4C_{xx}\langle S_z\rangle\sum_f \mathcal{J}_{fg}[G_E{}^-(f,l)+G_E{}^+(f,l)]+2[C_x+2C_{xz}\langle S_z\rangle\mathcal{J}(0)]G_E{}^z(g,l). \tag{3.21}$$

To obtain these equations we have used the following decoupling approximations in the RPA:

$$\langle\langle S_g{}^+S_{fz};S_l{}^-\rangle\rangle\to\langle S_z\rangle\langle\langle S_g{}^+;S_l{}^-\rangle\rangle, \tag{3.22a}$$

$$\langle\langle S_{gz}S_{fz};S_l{}^-\rangle\rangle\to\langle S_z\rangle\langle\langle S_{gz};S_l{}^-\rangle\rangle, \tag{3.22b}$$

$$\langle\langle S_g{}^+S_f{}^+;S_l{}^-\rangle\rangle,\quad\langle\langle S_g{}^+S_f{}^-;S_l{}^-\rangle\rangle\to 0. \tag{3.22c}$$

In Eqs. (3.20) and (3.21) a new quantity

$$G_E{}^z(g,l)\equiv\langle\langle S_{gz};S_l{}^+\rangle\rangle_E \tag{3.23}$$

appears. This shows the effect of an effective transverse static field on the system. However, Eq. (2.29), giving the RPA condition for the vanishing of such a transverse field, just causes the coefficient of this term to vanish.

Then taking the spatial Fourier transform of (3.30) and (3.31), one solves for the Green's functions. We obtain

$$G_E{}^-(k)=-\langle S_z\rangle(E+\beta)/\pi(E-E_k)(E+E_k), \tag{3.24}$$

$$G_E{}^+(k)=-\langle S_z\rangle\lambda/\pi(E-E_k)(E+E_k). \tag{3.25}$$

Here β and λ are given by (3.3) and (3.4), where for the finite-T behavior, $\langle S_z\rangle$ now denotes the thermal average, and E_k for the ordered phase is the same as in (3.8), so that the excitation spectrum at finite T is obtained from that at $T=0$ in the RPA by letting $\langle S_z\rangle$ denote the thermal average rather than the ground-state expectation value.

To obtain the value of $\langle S_z\rangle$, which self-consistently determines the excitation spectrum, we calculate the correlation function $\langle S_k{}^+S_k{}^-\rangle$ from the Green's func-

[11] D. N. Zubarev, Usp. Fiz. Nauk **71**, 71 (1960) [English transl.: Sov. Phys—Usp. **3**, 320 (1960)].

tions. We obtain

$$\langle S_k^+ S_k^-\rangle = -(\langle S_z\rangle/E_k)[(E_k+\beta)/(e^{(E_k/T)}-1) + (E_k-\beta)/(e^{(-E_k/T)}-1)]. \quad (3.26)$$

Then $\langle S_z\rangle$ is determined self-consistently by substituting this into the expression

$$\langle S_z\rangle = -\tfrac{1}{2}+\frac{1}{N}\sum_k \langle S_k^+ S_k^-\rangle. \quad (3.27)$$

This procedure gives

$$\langle S_z\rangle = -\frac{1}{2}\frac{1}{(\varphi_a+\Psi_a)}, \quad (3.28)$$

with

$$\varphi_a = \frac{1}{2N}\sum_k (1-a^2\gamma_k)^{-1/2}\coth(\epsilon_{k/2}), \quad (3.29)$$

$$\Psi_a = \frac{1}{2N}\sum_k (1-a^2\gamma_k)^{1/2}\coth(\epsilon_{k/2}), \quad (3.30)$$

where for the ordered phase

$$\mathcal{E}_k = E_k/T = (1-a^2\gamma_k)^{1/2}/t \quad (3.31)$$

and

$$t = Ta/\Delta. \quad (3.32)$$

Also, we obtain the corresponding self-consistent magnetization

$$\langle J\rangle/\alpha = -2\langle S_z\rangle(1-a^2)^{1/2}. \quad (3.33)$$

Equations (3.8), (3.9), (3.19), (3.29), (3.31), and (3.33) serve to self-consistently determine the excitation spectrum and the corresponding magnetization. The procedure is as follows: One fixes t/a. This is equivalent to fixing T/Δ, the ratio of the temperature to the crystal-field splitting. One then calculates φ_a and Ψ_a for a series of values of a by performing the lattice sums of (3.29) and (3.30). (This has been done for the simple cubic crystal by dividing the Brillouin zone into 4096 small cubes and taking the sums over the values of $\mathbf{k}$ at the center of the cubes. Using the symmetry properties of the simple cubic crystal, 165 distinct points, appropriately weighted, and occurring in 1/48 of the Brillouin zone are sufficient to do this.) Evaluation of these lattice sums is the main computational problem in the self-consistent determination of the magnetization and excitation spectrum. Then from (3.28) and (3.9), one finds $\langle S_z\rangle$ and A for each a. Thus, we calculate a curve of A versus a for fixed T. Hence, for a specified A, this curve gives us the value of a for the fixed T, and we also have the value of $\langle S_z\rangle$ for that a. Then, using (3.8) and (3.33), this allows us to fulfill our objective of self-consistently finding the excitation spectrum and the magnetization as a function of T for fixed A.

We also give here the generalization to finite temperature of (3.15), the RPA expression for the susceptibility. By exactly the same argument used for small H and, hence, for small θ at $T=0$, we obtain at all T:

$$\text{RPA, } \chi = (2\alpha^2 g^2\mu_B{}^2 k_B/\Delta)[-2\langle S_z\rangle/(1+2\langle S_z\rangle A)]. \quad (3.34)$$

4. TWO-SITE CORRELATION APPROXIMATION

The TSCA includes correlation effects between excitations on different sites. The use of this approximation in determining the excitation spectrum in the paramagnetic regime in the absence of applied field has been discussed in I. In the first part of this section, we complete the exposition of the way in which the TSCA is used at finite temperature for the paramagnetic regime in the absence of applied field. This completes the steps necessary for putting the results of I in a form suitable for self-consistent numerical calculations.

In the second part of this section, we apply the TSCA to a two-singlet-level system possessing a magnetic moment. We obtain the dispersion relation for the excitation waves in the ordered phase. The paramagnetic susceptibility is also calculated in the TSCA, and compared to that obtained in the RPA.

A. TSCA at Finite Temperature in Paramagnetic Regime in Absence of Applied Field

The present calculation continues from Eqs. (A39), (A40), (A42), and (A43) of I:

$$E_k/\Delta = [1+2\langle S_z\rangle A(\gamma_k-2\epsilon)]^{1/2}, \quad (4.1)$$

$$\xi = \Delta A\langle S_z\rangle(\gamma_k-2\epsilon), \quad (4.2)$$

$$\langle S_k^+ S_k^-\rangle = -(\langle S_z\rangle/E_k)[(E_k+\Delta+\xi)/(e^{(E_k/T)}-1) + (E_k-\Delta-\xi)/(e^{(-E_k/T)}-1)], \quad (4.3)$$

$$\langle S_k^+ S_{-k}^+\rangle = -(\langle S_z\rangle\xi/E_k)[-1/(e^{(E_k/T)}-1) + 1/(e^{(-E_k/T)}-1)], \quad (4.4)$$

where ϵ, as defined in (2.22), gives the effect of correlation between excitations on different lattice sites.

Define b by the relationship

$$A = b^2/-2\langle S_z\rangle(1-2b^2\epsilon), \quad (4.5)$$

so that

$$E_k/\Delta = (1-b^2\gamma_k)^{1/2}/(1-2b^2\epsilon)^{1/2}. \quad (4.6)$$

Then, using this expression in (4.3), from (3.27), we obtain $\langle S_z\rangle$ as

$$\langle S_z\rangle = -\tfrac{1}{2}(\Lambda_b\varphi_b+\Psi_b/\Lambda_b)^{-1}. \quad (4.7)$$

Here, φ_b and Ψ_b are given by (3.29) and (3.30), and

$$\mathcal{E}_k = E_k/T = (1-b^2\gamma_k)^{1/2}/t, \quad (4.8)$$

$$t = (T/\Delta)\Lambda_b, \quad (4.9)$$

$$\Lambda_b = (1-2b^2\epsilon)^{1/2}. \quad (4.10)$$

Equation (4.7) gives one relationship between $\langle S_z\rangle$ and ϵ. To determine $\langle S_z\rangle$ and ϵ requires a second such relationship. This is provided by the definition of ϵ in (2.22).

Consider first the

$$\frac{1}{N}\sum_k \gamma_k\langle S_k{}^+S_{-k}{}^+\rangle$$

term in (2.22). From (4.3), using Eq. (4.2) for ξ, and the definitions (4.8)–(4.10), one obtains

$$\frac{1}{N}\sum_k \gamma_k\langle S_k{}^+S_{-k}{}^+\rangle = -\langle S_z\rangle\left[\left(\frac{\Lambda_b}{2b^2}\right)(\varphi_b-\Psi_b)-\left(\frac{1}{2\Lambda_b}\right)\tilde{\Psi}_b\right] \quad (4.11)$$

with

$$\tilde{\Psi}_b=\frac{1}{N}\sum_k \gamma_k(1-b^2\gamma_k)^{1/2}\coth(\tfrac{1}{2}\epsilon_k). \quad (4.12)$$

Similarly,

$$\frac{1}{N}\sum_k \gamma_k\langle S_k{}^+S_k{}^-\rangle = -\langle S_z\rangle\left[\left(\frac{\Lambda_b}{2b^2}\right)(\varphi_b-\Psi_b)+\left(\frac{1}{2\Lambda_b}\right)\tilde{\Psi}_b\right], \quad (4.13)$$

so that

$$\epsilon=-\langle S_z\rangle(\Lambda_b/b^2)(\varphi_b-\Psi_b). \quad (4.14)$$

Equations (4.7) and (4.14) are then the basic equations self-consistently determining $\langle S_z\rangle$ and ϵ for the TSCA in the paramagnetic regime in the absence of applied field. In fact, using Eq. (4.7) one can eliminate $\langle S_z\rangle$, and using (4.10) one can eliminate ϵ from (4.14). Thus, one arrives at a quadratic equation for $\Lambda_b{}^2$ which has the solution

$$\Lambda_b{}^2=\Psi_b/\varphi_b. \quad (4.15)$$

From (4.9), using (4.5), one obtains

$$t/b=[-1/(2\langle S_z\rangle A)]^{1/2}(T/\Delta). \quad (4.16)$$

For fixed t/b, as b varies, T/Δ varies only slowly. We make use of this fact in setting up our self-consistent numerical procedure. A fixed value is chosen for t/b and b is varied. Then for each value of b, one determines Λ_b from (4.15), and, using (4.7) and (4.10), one then determines $\langle S_z\rangle$ and ϵ. Finally, from (4.5) one finds A, and from (4.16) one finds T/Δ. Consequently for specified A, one finds for each b the corresponding T/Δ, $\langle S_z\rangle$, and ϵ.

B. TSCA When the System Has A Magnetic Moment

As discussed in Sec. 2, in order to calculate the normal mode energies corresponding to small deviations of the pseudospin from its equilibrium position, we must first perform a rotation of the pseudospin coordinate axes by a small angle φ to eliminate the presence of any effective field transverse to the equilibrium axis. As already discussed, in the RPA such transverse field effects vanish automatically. However, in any improved treatment such as the TSCA, the rotation by φ must be performed. The rotation angle φ is determined from (2.27).

To calculate the paramagnetic susceptibility for small magnetic field we need only to consider the small θ and φ limit. It will be shown below that, to the first order in ϵ,

$$\varphi=-8A\langle S_z\rangle\epsilon\theta. \quad (4.17)$$

In the following, we shall first calculate the elementary excitation spectrum in the ordered phase. Then we consider the case when there is an applied magnetic field present in the paramagnetic regime, and we find the paramagnetic susceptibility in the TSCA.

a. Elementary Excitations in the Ordered Phase at $T=0$

To calculate the energy spectrum in the ordered phase at $T=0$, we consider the Fourier transformed equations of motion:

$$i\dot{S}_k{}^+=[S_k{}^+,\mathcal{H}]=-C_zS_k{}^+ +\sum_q \mathcal{J}(q) \times[-2C_{zz}S_{k-q}{}^+S_{qz}+4C_{xx}S_{k-qz}(S_q{}^+ +S_{-q}{}^-)], \quad (4.18)$$

where

$$S_k{}^{\pm}\equiv\frac{1}{\sqrt{N}}\sum_f S_f{}^{\mp}e^{\mp i\mathbf{k}\cdot\mathbf{r}_f},\quad S_{kz}\equiv\frac{1}{\sqrt{N}}\sum_f S_{fz}e^{-i\mathbf{k}\cdot\mathbf{r}_f}. \quad (4.19)$$

We recall that our treatment involves writing S_z in the form given in (2.19), which is exact. All approximations then involve the quantity in square brackets in (2.19), which is always small. To proceed, we first consider the Fourier transform of (2.18)

$$S_{kz}=\langle S_z\rangle\delta_{k0}+\Big[(\tfrac{1}{2}-\langle S_z\rangle)\frac{1}{N}\sum_{k_1} S_{k+k_1}{}^+S_{k_1}{}^- -(\tfrac{1}{2}+\langle S_z\rangle)\frac{1}{N}\sum_{k_1} S_{-k+k_1}{}^-S_{k_1}{}^+\Big]. \quad (4.20)$$

Then we make approximations on the products of $S_k{}^+$ and the operators in the square brackets. Thus, in the first term on the right-hand side in (4.17),

$$\sum_q \mathcal{J}(q)S_{k-q}{}^+S_{qz}=\langle S_z\rangle\mathcal{J}(0)S_k{}^+ +(\tfrac{1}{2}-\langle S_z\rangle)\frac{1}{N}\sum_{q,k_1}\mathcal{J}(q)S_{k-q}{}^+S_{q+k_1}{}^+S_{k_1}{}^- -(\tfrac{1}{2}+\langle S_z\rangle)\frac{1}{N}\sum_{q,k_1}\mathcal{J}(q)S_{k-q}{}^+S_{-q+k_1}{}^-S_{k_1}{}^+ \quad (4.21)$$

$$\approx\langle S_z\rangle\mathcal{J}(0)S_k^+ + (\tfrac{1}{2}-\langle S_z\rangle)\left[\frac{1}{N}\sum_{k_1}\mathcal{J}(0)S_k^+\langle S_{k_1}^+S_{k_1}^-\rangle + \frac{1}{N}\sum_{k_1}\mathcal{J}(k-k_1)S_k^+\langle S_{k_1}^+S_{k_1}^-\rangle + \frac{1}{N}\sum_{q}\mathcal{J}(q)\langle S_{k-q}^+S_{q-k}^+\rangle S_{-k}^-\right]$$

$$-(\tfrac{1}{2}+\langle S_z\rangle)\left[\frac{1}{N}\sum_{k_1}\mathcal{J}(0)S_k^+\langle S_{k_1}^-S_{k_1}^+\rangle + \frac{1}{N}\sum_{k_1}\mathcal{J}(k+k_1)\langle S_{-k_1}^+S_{k_1}^+\rangle S_{-k}^- + \frac{1}{N}\sum_{k_1}\mathcal{J}(q)\langle S_{k-q}^+S_{-q+k}^-\rangle S_k^+\right]. \quad (4.22)$$

For nearest-neighbor exchange interaction, it can be shown that

$$\sum_q \mathcal{J}(q)S_{k-q}^+S_{qz} \approx \langle S_z\rangle\mathcal{J}(0)S_k^+ - 2\langle S_z\rangle\mathcal{J}(k)\delta_1'S_k^+ - 2\langle S_z\rangle\mathcal{J}(k)\delta_2'S_{-k}^-, \quad (4.23)$$

where

$$\delta_1' = \frac{1}{N}\sum_k \gamma_k\langle S_k^+S_k^-\rangle, \quad (4.24a)$$

$$\delta_2' = \frac{1}{N}\sum_k \gamma_k\langle S_k^+S_{-k}^+\rangle. \quad (4.24b)$$

Similarly,

$$\sum_q \mathcal{J}(q)S_{k-qz}S_q^+ \approx \langle S_z\rangle\mathcal{J}(k)S_k^+ - 2\langle S_z\rangle\mathcal{J}(0)\delta_1'S_k^+ - 2\langle S_z\rangle\mathcal{J}(0)\delta_2'S_{-k}^-. \quad (4.25)$$

Then the equation of motion becomes

$$i\dot{S}_k^+ = -\beta'S_k^+ + \lambda'S_{-k}^-, \quad (4.26)$$

with

$$\beta' = C_z + 2C_{zz}\langle S_z\rangle\mathcal{J}(0) - 4C_{zz}\langle S_z\rangle\mathcal{J}(k)\delta_1' - 4C_{xx}\langle S_z\rangle\mathcal{J}(k) + 8C_{xx}\langle S_z\rangle\mathcal{J}(0)\epsilon, \quad (4.27a)$$

$$\lambda' = 4C_{zz}\mathcal{J}(k)\delta_2' + 4C_{xx}\langle S_z\rangle\mathcal{J}(k) - 8C_{xx}\langle S_z\rangle\mathcal{J}(0)\epsilon. \quad (4.27b)$$

Similarly,

$$i\dot{S}_{-k}^- = \beta'S_{-k}^- - \lambda'S_k^+. \quad (4.28)$$

So the excitation spectrum is

$$E_k = \{[C_z + 2C_{zz}\langle S_z\rangle\mathcal{J}(0) - 4C_{zz}\langle S_z\rangle\mathcal{J}(k)(\delta_1' - \delta_2')] \times [C_z + 2C_{zz}\langle S_z\rangle\mathcal{J}(0) - 4C_{zz}\langle S_z\rangle\epsilon\mathcal{J}(k) - 8C_{xx}\langle S_z\rangle\mathcal{J}(k) + 16C_{xx}\langle S_z\rangle\mathcal{J}(0)\epsilon]\}^{1/2}. \quad (4.29)$$

If we define

$$\tilde{a} \equiv \Delta/-8\langle S_z\rangle\mathcal{J}(0)\alpha^2(1-2\epsilon), \quad (4.30)$$

the coefficients given in (2.29) can be written as

$$C_z = \Delta\tilde{a}, \quad (4.31a)$$

$$C_{zz} = -4\alpha^2(1-\tilde{a}^2), \quad (4.31b)$$

$$C_{xx} = -\alpha^2\tilde{a}^2. \quad (4.31c)$$

Inserting these into (4.29), we obtain

$$E_k = -8\langle S_z\rangle\mathcal{J}(0)\alpha^2\{[1-2\epsilon\tilde{a}^2 - 2\tilde{\epsilon}(1-\tilde{a}^2)\gamma_k] \times [1-(\tilde{a}^2+(1-\tilde{a}^2)2\epsilon)\gamma_k]\}^{1/2}, \quad (4.32)$$

where we have defined another quantity

$$\tilde{\epsilon} = \delta_1' - \delta_2'. \quad (4.33)$$

Then, (4.32) gives the elementary excitation spectrum in the ferromagnetic ordered phase. The magnetic moment, given by (2.15), can be expressed as

$$\langle J\rangle = -2\alpha\langle S_z\rangle(1-\tilde{a}^2)^{1/2}. \quad (4.34)$$

b. Green's-Function Formalism for Ordered Phase at Finite Temperature

To study the finite-temperature behavior in the ferromagnetic regime, we use the Green's-function formalism. The procedure is completely in parallel to that of Sec. 3 B for the RPA. The two types of Green's function are defined as in (3.18) and (3.19). If we adopt the approximations shown in Eqs. (2.20)–(2.21b), the coefficient of the new Green's function $\langle\langle S_{iz}(t); S^-(0)\rangle\rangle_E$ vanishes according to the condition (2.24) for vanishing effective field discussed in Sec. 2. We recall that the coefficients C_x, C_z, C_{zz}, etc., have been given in (2.26).

Using Callen's decoupling instead of the RPA,

$$\langle\langle S_g^-S_{jz}; S_l^-\rangle\rangle \underset{g\neq j}{\rightarrow} \langle S_z\rangle\langle\langle S_g^-; S_l^+\rangle\rangle - 2\langle S_z\rangle\langle S_g^-S_j^+\rangle\langle\langle S_j^-; S_l^+\rangle\rangle - 2\langle S_z\rangle\langle S_g^-S_j^-\rangle\langle\langle S_j^+; S_l^+\rangle\rangle, \quad (4.35)$$

and completing the spatial Fourier transformation as in the RPA, we obtain

$$G_E^-(k) = -(\langle S_z\rangle/\pi)(E+\beta')/(E-E_k)(E+E_k), \quad (4.36)$$

$$G_E^+(k) = -(\langle S_z\rangle/\pi)[\lambda'/(E-E_k)(E+E_k)], \quad (4.37)$$

with β' and λ' defined in Eqs. (4.25a) and (4.25b), and E_k given in (4.32)

The corresponding correlation functions obtained from the Green's functions are

$$\langle S_k^+S_k^-\rangle = -\langle S_z\rangle[-1+(\beta'/E_k)\coth(E_k/2T)], \quad (4.38)$$

$$\langle S_k^+S_{-k}^+\rangle = -\langle S_z\rangle(\lambda/E_k)\coth(E_k/2T). \quad (4.39)$$

These then enable us to find $\langle S_z\rangle$, as in the RPA, and δ_1', δ_2' (or consequently ϵ and $\tilde{\epsilon}$) self-consistently. The calculational procedure is much more complicated than that in the RPA because of the more complicated dispersion relationship and the appearance of $\tilde{\epsilon}$. However, we shall analyze the high-temperature behavior in Sec. 6 to examine the phase transition.

c. Paramagnetic Susceptibility in TSCA

From (2.15)

$$\langle J\rangle = -2\alpha\langle S_{z'}\rangle\sin(2\theta-\varphi), \quad (4.40)$$

where θ is given by (2.8), and φ is given by (2.27). We use z' to denote the rotated coordinate axis, where there is no transverse effective field.

In the paramagnetic phase $\langle J\rangle$, and hence θ, tend to 0 as $H\to 0$. Then for an infinitesimal magnetic field, retaining only first-order terms, in θ, from (2.27) we have

$$(2\theta-\varphi)[1+8\langle S_{z'}\rangle\mathcal{J}(0)\alpha^2(1-2\epsilon)/\Delta -2g\mu_B\alpha H/\Delta]=0. \quad (4.41)$$

From (4.40) and (2.8), we have

$$\langle J\rangle=-2\langle S_{z'}\rangle\alpha(2\theta-\varphi) \quad (4.42)$$

and

$$2\theta=4\mathcal{J}(0)\alpha\langle J\rangle/\Delta+2g\mu_B\alpha H/\Delta. \quad (4.43)$$

Combining Eqs. (4.42) and (4.43),

$$2\theta=-[8\langle S_{z'}\rangle\mathcal{J}(0)\alpha^2/\Delta](2\theta-\varphi)+2g\mu_B\alpha H/\Delta. \quad (4.44)$$

We can then eliminate the H term from Eqs. (4.41) and (4.44) and solve for φ. We obtain

$$\varphi=-8A\langle S_{z'}\rangle\epsilon\theta/(1-4A\langle S_{z'}\rangle\epsilon). \quad (4.45)$$

Substituting this relationship into Eq. (4.42) and using (4.43), we solve for $\langle J\rangle$:

$$\langle J\rangle=(2g\mu_B\alpha^2/\Delta)(-2\langle S_{z'}\rangle)H/(1-1/\tilde{a}), \quad (4.46)$$

where we recall from (4.30) that

$$\tilde{a}=\Delta/-8\langle S_{z'}\rangle\mathcal{J}(0)\alpha^2(1-2\epsilon). \quad (4.47)$$

The susceptibility is obtained as

$$\chi=(2g^2\mu_B{}^2\alpha/\Delta)(-2\langle S_{z'}\rangle)/(1-1/\tilde{a}). \quad (4.48)$$

There is a slight difference between $\langle S_{z'}\rangle$ and $\langle S_z\rangle$. However,

$$\langle S_{z'}\rangle=\langle S_z\rangle\cos\varphi-\langle S_x\rangle\sin\varphi, \quad (4.49)$$

where

$$\langle S_x\rangle=\langle S_{z'}\rangle\sin\varphi+\langle S_{x'}\rangle\cos\varphi=\langle S_{z'}\rangle\sin\varphi, \quad (4.50)$$

since $\langle S_{x'}\rangle=0$.

Since $\varphi\approx 4A\epsilon\theta$, $\langle S_{z'}\rangle$ differs from $\langle S_z\rangle$ by a quantity of order $(4A\epsilon\theta)^2$, and we can replace $\langle S_{z'}\rangle$ by $\langle S_z\rangle$. Therefore, in the TSCA formula for the susceptibility, (4.48), $\langle S_{z'}\rangle$ is replaced by $\langle S_z\rangle$, and $\langle S_z\rangle$ and ϵ are the quantities calculated in the paramagnetic phase without field as in Sec. 4 A.

5. SPECIFIC HEAT

In this section we give the expressions for the RPA specific heat in the ferromagnetic and paramagnetic regimes, and for the TSCA specific heat in the paramagnetic regime. The results can be compared to the molecular-field-theory behavior, and this is discussed in Sec. 6.

A. Paramagnetic Regime

The internal energy is

$$U=\langle\mathcal{H}\rangle, \quad (5.1)$$

where

$$\mathcal{H}=\sum_i \Delta S_{iz}-\sum_{\langle i,j\rangle}\mathcal{J}_{ij}\alpha^2(2S_i{}^+S_j{}^-+S_i{}^+S_j{}^++S_i{}^-S_j{}^-). \quad (5.2)$$

Then Fourier transforming and taking the thermal average gives

$$U=N\Delta\langle S_z\rangle+2\alpha^2\mathcal{J}(0)\sum_k\gamma_k(\langle S_k{}^+S_k{}^-\rangle+\langle S_k{}^+S_{-k}{}^+\rangle), \quad (5.3)$$

or, per mole (recalling that our unit of energy is Boltzmann's constant)

$$U/R\Delta=\langle S_z\rangle+(\tfrac{1}{2}A)\epsilon. \quad (5.4)$$

One has the RPA and TSCA depending on whether one sets the ϵ term equal to zero or not in determining the collective excitation spectrum. The specific heat

$$C_v=dU/dT \quad (5.5)$$

is obtained by calculating U, and finding the derivative with respect to temperature numerically.

For comparison, the corresponding expressions in molecular-field theory are

$$\text{molecular-field theory, } U/R\Delta=-\tfrac{1}{2}\tanh(\Delta/2T), \quad (5.6)$$

$$\text{molecular-field theory, } C_v/R=(\Delta/2T)^2\operatorname{sech}^2(\Delta/2T). \quad (5.7)$$

B. Ferromagnetic Regime

$$\mathcal{H}=\sum_i C_zS_{iz}+\sum_i 2(C_x-\mathcal{J}(0)C_{xz})S_{ix} +2\sum_{\langle i,j\rangle}\mathcal{J}_{ij}C_{xz}(S_i{}^++S_i{}^-)S_j{}^+S_j{}^-+\sum_{\langle i,j\rangle}\mathcal{J}_{ij} \times[C_{zz}S_{iz}S_{jz}+C_{xx}(S_i{}^++S_i{}^-)(S_j{}^++S_j{}^-)]. \quad (5.8)$$

Then,

$$U=\langle\mathcal{H}\rangle=NC_z\langle S_z\rangle+\sum_{\langle i,j\rangle}\mathcal{J}_{ij}C_{zz}\langle S_{iz}S_{jz}\rangle +\sum_{\langle i,j\rangle}\mathcal{J}_{ij}C_{xx}\langle(S_i{}^++S_i{}^-)(S_j{}^++S_j{}^-)\rangle. \quad (5.9)$$

Using the explicit expressions for C_z and C_{zz} in the RPA and the approximation that $\langle S_{iz}S_{jz}\rangle\approx\langle S_z\rangle^2$, one obtains

$$\text{RPA,}\quad U/R\Delta\approx-(1/4A)-A\langle S_z\rangle^2-\epsilon/8\langle S_z\rangle^2A, \quad (5.10)$$

and the specific heat is found by taking the derivative with respect to temperature.

For comparison, for the ferromagnetic regime in molecular-field theory

$$U/R=-(\Delta/2\cos2\theta)\tanh(\Delta/2T\cos2\theta), \quad (5.11)$$

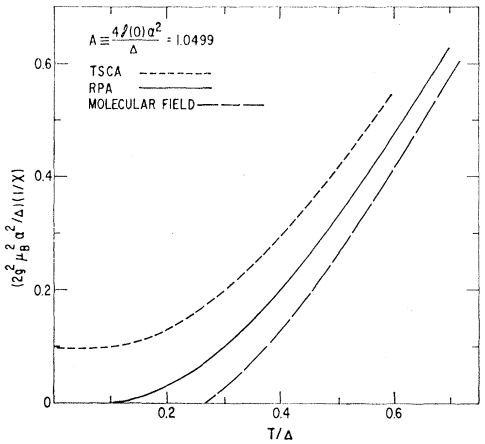

FIG. 1. Inverse susceptibility versus temperature of the two-singlet-level system for simple cubic lattice with nearest-neighbor ferromagnetic exchange. The value of $A \equiv 4\mathcal{J}(0)\alpha^2/\Delta$ is such that $T_c/\Delta = 0.269$ in the molecular-field approximation, $T_c/\Delta = 0.10$ in the RPA, and the system never orders magnetically in the TSCA. (See Ref. 12.)

where θ is determined by solving the equation

$$1/A \cos 2\theta = \tanh(\Delta/2T \cos 2\theta). \qquad (5.12)$$

To explicitly demonstrate the contribution to the specific heat due to the ϵ term in (5.4), we neglect this term in the RPA calculations discussed in Sec. 6 below, while the ϵ is included in the TSCA calculation.

6. RESULTS OF NUMERICAL CALCULATIONS AND DISCUSSION

A. Susceptibility and Magnetization

The critical value of A in the RPA for ferromagnetic ordering with infinitesimal moment at $T=0$ is 1.0406. In Fig. 1, we show the behavior of the inverse susceptibility in the paramagnetic regime for a value of A only slightly greater than this RPA critical value. (For simplicity, the calculations shown in this and all subsequent figures were performed for the simple cubic lattice with nearest-neighbor ferromagnetic exchange.) In particular, T_c/Δ in the RPA for this A is 0.1. The values of $1/\chi$ in the TSCA and in the molecular-field approximation are shown for the same A. The TSCA curve[12] lies substantially above the RPA curve for low T, and approaches the RPA and molecular-field curves at high T. Thus in the paramagnetic regime, the TSCA curve of $1/\chi$ versus T is "flatter" than the RPA curve. This "flattening," caused by correlation effects, has been noted by Cooper[4] for a constant-coupling calculation. There is no downward dip at low T in the curve of $1/\chi$ versus T as was observed experimentally[4,13] in TmN. The present results combined with the earlier results for the constant-coupling calculation lead us to believe that the downward dip found experimentally in TmN can probably be attributed to the chemical quality of the sample, rather than to any fundamental mechanism associated with exchange effects.

In Fig. 2, we show the variation of the collective excitation spectrum with temperature in the RPA for the same value of A. In the ferromagnetic regime, as T/Δ increases from zero, the $\mathbf{k}=0$ mode energy drops toward zero. The rate of decrease is, however, slow until T is close to the Curie temperature, whereupon the $\mathbf{k}=0$ mode frequency drops to zero precipitously. For T greater than the Curie temperature, the mode frequency increases again. For high temperatures, the collective excitation energies approach Δ (the crystal-field-only splitting between the two-singlet levels), and the dispersion tends to disappear.

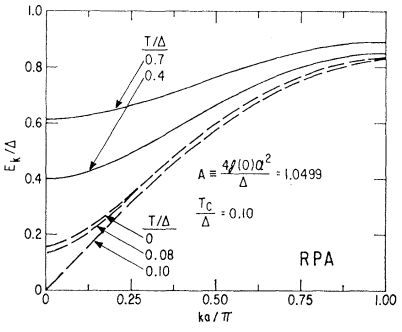

FIG. 2. Variation with temperature of the dispersion curve of elementary excitations in the RPA for exchange such that $T_c/\Delta = 0.10$.

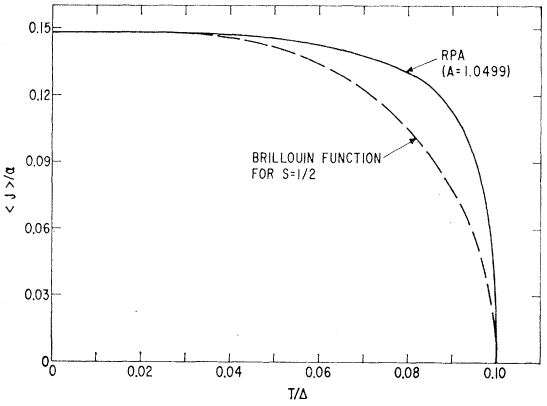

FIG. 3. Thermal variation of magnetization in the RPA for two-singlet-level system with $T_c/\Delta = 0.10$.

[12] The fact, discussed below, that the magnetic transition at $T=0$ is first order in the TSCA (i.e., in a plot of $\langle J \rangle/\alpha$ versus A, there is a discontinuity when $\langle J \rangle$ becomes nonzero), makes it difficult to fix the critical value of A for which magnetic ordering first occurs at $T=0$. The critical value, $A=1.1852$, found in I for ordering with infinitesimal magnetic moment at $T=0$ only provides an upper limit to A_{crit} for a first-order transition. Thus, it is possible that for the value $A=1.0406$, used in Fig. 1, in the TSCA there is a first-order magnetic transition at sufficiently low T (and the curve for $1/\chi$ would be inapplicable below that T). However, the A used in Fig. 1 is probably sufficiently small so that one never has magnetic ordering in the TSCA.

[13] B. R. Cooper, I. S. Jacobs, R. C. Fedder, J. S. Kouvel, and D. P. Schumacher, J. Appl. Phys. 37, 1384 (1966).

As described in Sec. 3, from the self-consistent determination of the excitation behavior, we also find the temperature dependence of the magnetization in the RPA. As shown in Fig. 3, the most striking feature is the sharp drop in magnetization close to the Curie temperature. This corresponds to the precipitous drop in the $\mathbf{k}=0$ mode energy near T_c. As shown in Fig. 4, for this value of A, only slightly above the RPA critical value, there is a large difference between the RPA magnetization and the molecular-field magnetization behavior.

As T_c/Δ increases, the RPA magnetization is discontinuous at T_c. The discontinuity is most significant for values of T_c/Δ near unity, where, as shown[14] in Fig. 5, it is quite substantial. As shown in Fig. 6, the excitation spectrum is considerably narrower than for lower T_c.

As T_c/Δ increases still further in the RPA, while the discontinuity in magnetization persists, the size of discontinuity decreases, and the magnetization approaches

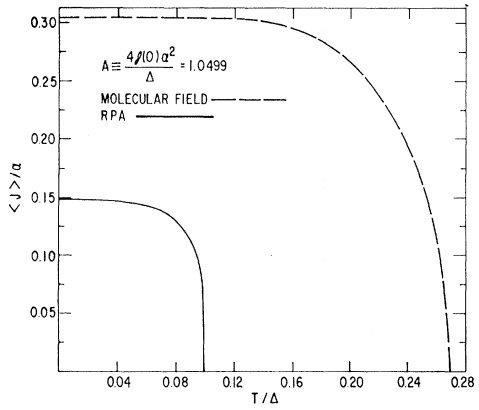

FIG. 4. Comparison of magnetization in RPA and molecular-field approximation for $A \equiv 4\mathcal{J}(0)\alpha^2/\Delta = 1.0499$. (Saturation value of magnetization for model two-singlet-level system, i.e., "model free-ion moment," is $\langle J \rangle/\alpha = 1$.)

the molecular-field behavior. This is shown in Fig. 7 for $T_c/\Delta = 5$. (For some range of T below T_c in both Figs. 5 and 7, the calculations give a double-valued magnetization. As discussed below, we attach physical significance to the upper branch. The lower unphysical solution for the magnetization is shown as a short dashed curve.) The corresponding excitation spectrum, shown in Fig. 8,

[14] The magnetization curves of Figs. 5 and 7 show the lower limit of the magnetization discontinuity at the first-order transition (i.e., they show the transition occurring at the extreme point of the $\langle J \rangle/\alpha$-versus-T/Δ curves, where the upper and lower branches coincide). The argument presented here does not preclude the possibility of the first-order transition occurring at a lower temperature where the two branches do not coincide. (Of course, even if free-energy considerations indicate that the first-order transition occurs at a temperature below the T_c of Fig. 5 or 7, the necessary nucleation processes may not occur, and a metastable situation may prevail, with the actual transition occuring at any temperature up to the T_c shown.) We are grateful to Dr. M. Blume for bringing this possibility to our attention.

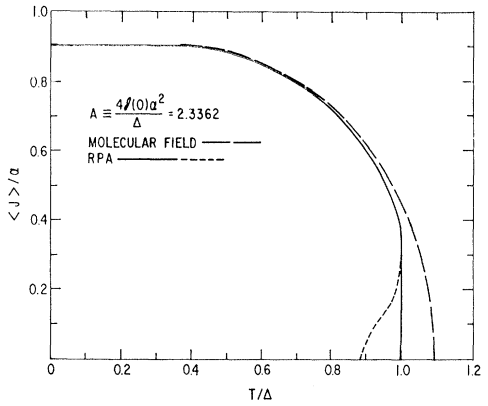

FIG. 5. Comparison of magnetization in RPA and molecular-field approximation for $A = 4\mathcal{J}(0)\alpha^2/\Delta = 2.3362$.

becomes quite flat. This is consistent with the molecular-field behavior for the magnetization.

The approach to molecular-field behavior in the RPA for large exchange is easily understood. First, we point out that there are no spin waves in our induced moment system even if we allow $A \to \infty$. This is because the two states of a single ion go to $|\pm m\rangle$ with $m > \frac{1}{2}$ in our model as $A \to \infty$. [Here m denotes the J_z quantum number. For example, for Pr^{3+} in a hexagonal crystal field, the two lowest-singlet states are $1/\sqrt{2}(|+3\rangle - |-3\rangle)$ and $1/\sqrt{2}(|+3\rangle + |-3\rangle)$. As exchange increases from zero, these states mix, and in the limit of large exchange, the states become $|+3\rangle$ and $|-3\rangle$.] The spin waves involve transitions to $|m \pm 1\rangle$, and these are higher lying states not taken into account for our model system. Second, as $A \to \infty$, there are also no excitations of the type we have considered, since the coupling vanishes between the two single-ion states, i.e., $\langle m|J_z|-m\rangle = 0$.

As shown[14] in Figs. 5 and 7, the presence of a first-order transition at T_c is associated with the presence of a lower "unphysical" branch to the magnetization curve for some range of T below T_c. We can now discuss

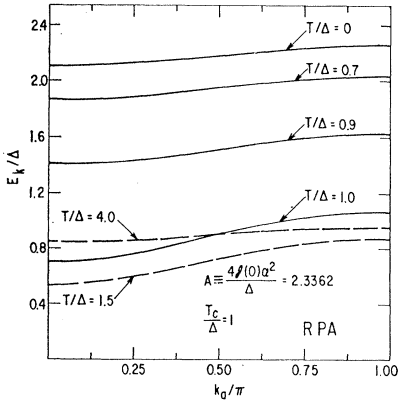

FIG. 6. Thermal variation of excitation spectrum in RPA for $A \equiv 4\mathcal{J}(0)\alpha^2/\Delta = 2.3362$.

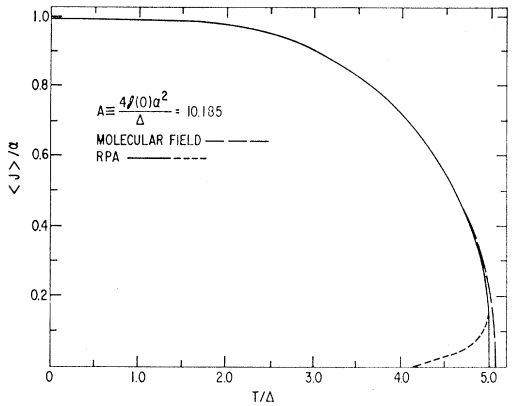

FIG. 7. Comparison of magnetization in RPA and molecular-field approximation for $A \equiv 4\mathcal{J}(0)\alpha^2/\Delta = 10.185$.

why we attach physical significance to the upper of the two branches of the magnetization curve in that temperature range (i.e., why the free energy is lower for the upper branch).

We recall from the discussion of Sec. 3, that we find the self-consistent ferromagnetic behavior in the RPA by performing the calculations for a succession of fixed values of T. For each fixed T, we vary a, calculate $\langle S_z\rangle$, and find A as a function of a from the relationship

$$\text{RPA ferromagnet, } a = -1/(2\langle S_z\rangle A). \tag{6.1}$$

When we do this, we find (as shown in Fig. 9) that for some range of a, a is a double-valued function of A. Since the magnetization is given by (3.33) as

$$\langle J\rangle/\alpha = -2\langle S_z\rangle(1-a^2)^{1/2}, \tag{6.2}$$

this in turn means that for fixed T, for some range of A (as illustrated in Fig. 10), $\langle J\rangle$ is a double-valued function of A. When translated to a plot of $\langle J\rangle$ versus T, this gives the double-branched behavior of the magnetization for a range of T below T_c.

This is in distinction to the molecular-field behavior,[3] where $\langle J\rangle$ is also given by (6.2) and (6.1), but where for specified a at fixed T, $\langle S_z\rangle$ differs from the RPA value. In Bleaney's[3] notation

$$\text{molecular field, } -2\langle S_z\rangle \equiv 2p-1 = \tanh(W/2T), \tag{6.3}$$

where W is the molecular-field energy splitting and is equal to Δ/a. For the molecular-field treatment, A decreases monotonically with increasing a at fixed T. This in turn means that $\langle J\rangle$ decreases monotonically with A at fixed T, and the magnetic transition is second order as shown in Figs. 9 and 10.

Mathematically, the double-valued behavior of a for some range of A in the RPA can be understood by considering the behavior of the excitation spectrum given by (3.8)

$$E_k/\Delta = (1/a)(1-a^2\gamma_k)^{1/2} \tag{6.4}$$

as a increased from zero to unity. In particular, the double-valued character arises because of the rapid rate at which the fractional population of the molecular-field ground state, $p=\frac{1}{2}-\langle S_z\rangle$ decreases at fixed T as a increases from zero to unity. This rate is more rapid than in the molecular-field theory because not only the splitting of the two molecular-field levels (between which excitations arise) decreases as a increases, but also the gap in the excitation spectrum at $\mathbf{k}=0$ decreases. We therefore expect p to decrease faster than the rate given by molecular-field theory. [From (6.1), we see that A can go through a minimum for increasing a, if the rate of decrease of $|\langle S_z\rangle|$ becomes sufficiently rapid. Thus, we see how a nonmonotonic variation of A with a can occur in our calculations.]

In fact, if we consider the case of $T/\Delta \gg 1$, we can see the picture immediately. At this limit, in molecular-field theory,

$$\text{molecular field, } -2\langle S_z\rangle = \tanh(\Delta/2aT) \approx \Delta/2aT \quad (\text{for } a\neq 0) \tag{6.5}$$

and

$$A = 1/(-2\langle S_z\rangle a) = 2T/\Delta. \tag{6.6}$$

Therefore A is essentially independent of a, and a horizontal straight line is expected in the A-versus-a plot. (Such behavior occurs in Fig. 9 with $T/\Delta=10$ for the higher values of a.) On the other hand, in the RPA, admitting the collective excitations, we have, from Eqs. (3.28)–(3.32), in the limit of $\mathcal{E}_k \ll 1, (T/\Delta \gg 1)$

$$\text{RPA, } \quad -2\langle S_z\rangle = \Delta/2aTQ \tag{6.7}$$

with

$$Q \equiv \frac{1}{2N}\sum_k \left(\frac{1}{1-a^2\gamma_k}+1\right) \tag{6.8}$$

and

$$A = (2T/\Delta)Q. \tag{6.9}$$

Q is an increasing function of a and is always greater than unity for $1 \geq a > 0 (Q=1$ at $a=0$; $Q=1.207$ at at $a=1$ for the simple cubic lattice). Consequently at high T/Δ, A becomes a monotonically increasing

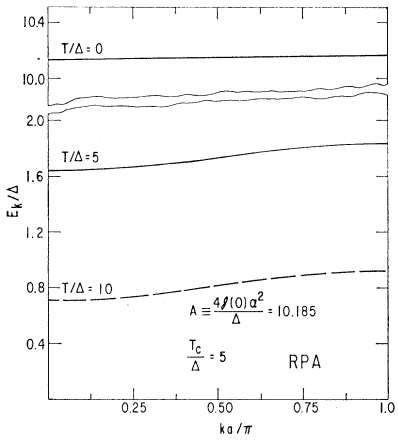

FIG. 8. Thermal variation of excitation spectrum in RPA for $A \equiv 4\mathcal{J}(0)\alpha^2/\Delta = 10.185$.

function of a. Combining this with the fact that at $T=0$, A is a monotonically decreasing function of a, we expect, for intermediate values of T/Δ, to find a minimum on the A-versus-a curve such as we actually obtained in Fig. 9.

While the self-consistent calculational procedure gives a nonmonotonic variation of A with a, physically by the following reasoning we may expect A to be a monotonically decreasing function of a. If the system is ordered, further increasing the exchange constant $\mathcal{J}$ (keeping T and Δ fixed) should result in increasing p. As $\mathcal{J}$ goes to ∞, we expect every ion to be in its ground state, and $p=1$. Now it is also clear (from the behavior of the energy spectrum) that p is a monotonically decreasing function of a. We therefore conclude that A is expected to be a montonically decreasing function of a.

As already stated, in contrast to this physically expected behavior for our calculational procedure in the RPA there is a value of a (at finite T) such that beyond that value, A becomes an increasing function of a. We claim that this behavior is unphysical, and that this branch of the (a,A) curve is to be discarded.

In fact, if we did the calculation in another way, which is more complicated, by setting a value of $\mathcal{J}$ or A and solving the equation

$$Aa=\frac{1}{2N}\sum_k \frac{2-a^2\gamma k}{(1-a^2\gamma_k)^{1/2}}\coth\left(\frac{\Delta(1-a^2\gamma_k)^{1/2}}{2Ta}\right) \quad (6.10)$$

for a, we would obtain two values of a corresponding to two possible states. The state with higher a value (much lower magnetic moment) evidently has higher free energy. This picture is even clearer for $T/\Delta\gg 1$ or $\Delta\rightarrow 0$. The unphysical branch then is exactly the vanishing moment solution which is familiar in the molecular-field theory of ordinary ferromagnets. (The physical branch is given by $a=0$, and the theory reduces to the molecular-field theory as discussed previously.)

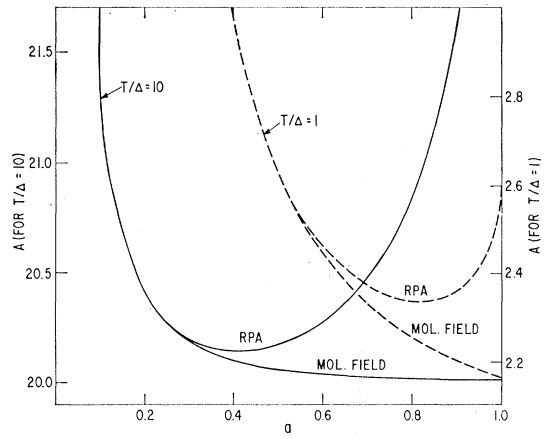

FIG. 9. Variation of $A\equiv 4\mathcal{J}(0)a^2/\Delta$ with a for fixed T/Δ in RPA and molecular-field approximation.

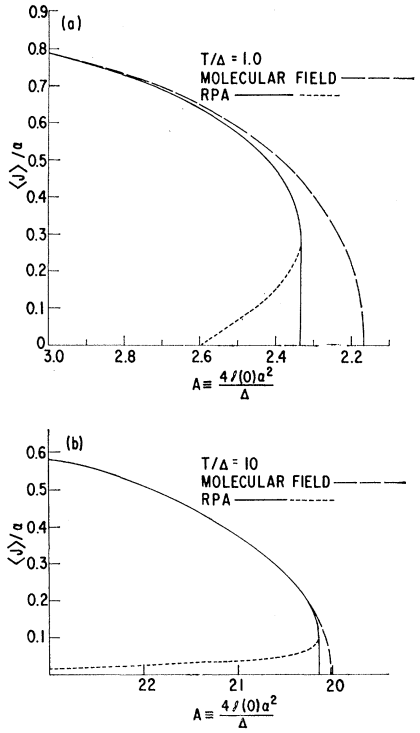

FIG. 10. Variation of magnetization with A for fixed T/Δ in RPA and molecular-field approximation.

The first-order transition occurs because the self-consistent behavior gives a minimum in the A-versus-a curve at some $a<1$. We have seen that physically this behavior arises because $|\langle S_z\rangle|$ falls off more rapidly with increasing a than in a molecular-field theory. This in turn occurs because the excitation waves, for a given magnetization give states of lower energy than the molecular-field excited state to serve as channels of depopulation of the ground state.

Our criterion that the magnetic transition at a specified T is first order (that there is a minimum in the A versus a curve for that T at some a between 0 and 1) allows us to find the value of T_c/Δ above, which the magnetic transition is first order. We do this by evaluating $dA/da|_{a=1}$. If this derivative is positive, this indicates the presence of a minimum in the A-versus-a curve. We find that $dA/da|_{a=1}$ is negative for $T/\Delta<0.1$, and changes sign at $T/\Delta\approx 0.1$ to become positive for $T/\Delta>0.1$. This indicates that for $T_c/\Delta<0.1$ the magnetic transition in the RPA is second order, while, for $T_c/\Delta\geq 0.1$ the transition is first order.

In the TSCA, a similar discontinuity of magnetization occurs. Although we did not carry out a general self-consistent calculation in this theory, for high values of T_c/Δ we can argue in a similar way to that given above for the RPA by exploring the $T/\Delta\gg 1$ behavior of the system. As discussed in Sec. 4, the magnetic moment is given as

$$\langle J\rangle=-2\alpha\langle S_z\rangle(1-\tilde{a}^2)^{1/2}, \quad (6.11)$$

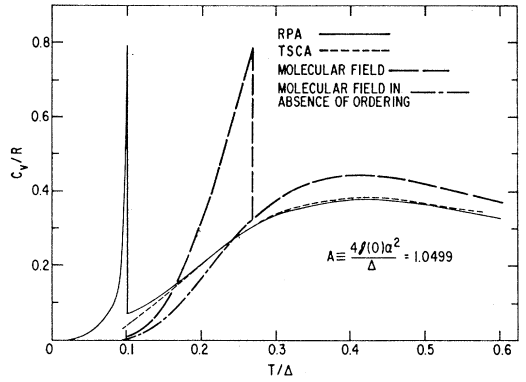

FIG. 11. Thermal variation of specific heat for two-singlet-level system for $A \equiv 4\mathcal{J}(0)\alpha^2/\Delta = 1.0499$. For the molecular-field calculation, in the paramagnetic regime C_v is independent of A, and we show the complete curve giving the Schottky anomaly if there were no magnetic transition.

where we recall

$$\tilde{a} = -1/2\langle S_z\rangle A(1-2\epsilon). \tag{6.12}$$

If the self-consistent calculation gives a maximum physical value of $\tilde{a}$ less than unity for fixed T/Δ and varying $\mathcal{J}$ (i.e., the minimum in the curve of A versus $\tilde{a}$ comes at $0<\tilde{a}<1$), we then have the discontinuous drop of magnetization at $\mathcal{J}_{\rm crit}$ (for fixed T/Δ) or at T_c(for fixed $\mathcal{J}/\Delta$).

To see this, we examine the case of $T/\Delta \gg 1$. We first observe that $\tilde{\epsilon}=0$. To show this we replace $\coth(E_k/2T)$ by $(2T/E_k)$ in Eqs. (4.38) and (4.39) and get,

$$\tilde{\epsilon} = \frac{1}{N}\sum_k \gamma_k(\langle S_k^+ S_k^-\rangle - \langle S_k^+ S_{-k}^+\rangle)$$

$$= \frac{T}{4\mathcal{J}(0)\alpha^2}\frac{1}{N}\sum_k \frac{\gamma_k}{1-2\epsilon\tilde{a}^2-2\tilde{\epsilon}(1-\tilde{a}^2)\gamma_k}. \tag{6.13}$$

$\tilde{\epsilon}=0$ is obviously a solution of the above equation, since

$$\sum_k \gamma_k = 0.$$

One can seek other solutions for $\tilde{\epsilon}$ by expanding the denominator in the summation and retaining only the low-order terms in ϵ and $\tilde{\epsilon}$ (since ϵ and $\tilde{\epsilon}$ are expected to be small). On doing this we see no acceptable solution for $\tilde{\epsilon}$ except $\tilde{\epsilon}=0$. We next calculate $\langle S_z\rangle$ and ϵ. This is done similarly to the calculation in the RPA. In the limit of $T/\Delta \gg 1$ (or more exactly $aT/\Delta \gg 1$), we have

$$-2\langle S_z\rangle = \frac{1}{T}\left\{\frac{1}{N}\sum_k\left(\frac{1}{\beta'-\lambda'}+\frac{1}{\beta'+\lambda'}\right)\right\}^{-1}, \tag{6.14}$$

$$\epsilon = -2\langle S_z\rangle T\frac{1}{N}\sum_k \frac{\gamma_k}{\beta'-\lambda'}. \tag{6.15}$$

Inserting β' and λ' from (4.30) and (4.34), these equations become

$$\Delta/(-2\langle S_z\rangle T(1-2\epsilon)\tilde{a}) = 1/(1-2\epsilon\tilde{a}^2)+(1+\Lambda Q_\Lambda), \tag{6.16}$$

$$\Delta\epsilon/(-\langle S_z\rangle T(1-2\epsilon)\tilde{a}) = 2Q_\Lambda, \tag{6.17}$$

where

$$\Lambda = \tilde{a}^2+(1-\tilde{a}^2)2\epsilon \tag{6.18}$$

and

$$Q_\Lambda = \frac{1}{N}\sum_k\left(\frac{\gamma_k}{1-\Lambda\gamma_k}\right). \tag{6.19}$$

For fixed $T/\Delta \gg 1$, we can solve for $\langle S_z\rangle$ and ϵ as functions of $\tilde{a}$, and therefore find $A = 1/(-2\langle S_z\rangle(1-2\epsilon)\tilde{a})$ as a function of $\tilde{a}$. We find that A is a monotonically *increasing* function of $\tilde{a}$ for $1\geq\tilde{a}>0$ in this high-temperature limit. As we have discussed, physical considerations require A to be a monotonically decreasing function of $\tilde{a}$. Therefore, for high Curie temperatures the only allowed value of $\tilde{a}$ is $\tilde{a}=0$, and the theory reduces to molecular-field theory in this case. For intermediate values of T/Δ we then expect a minimum in the A-versus-$\tilde{a}$ curve at some value of $\tilde{a}$ with $0<\tilde{a}_{\rm min}<1$. The physical regime of behavior then corresponds to values of $\tilde{a}$ between 0 and $a_{\rm min}$. Since $\tilde{a}$ cannot go to one, the magnetization cannot go continuously to zero. We therefore conclude that in the TSCA we obtain a first-order phase transition.

In fact, for the TSCA we can show that the magnetic transition is first order even at $T=0$. That is, at $T=0$ as one increases A from zero, the magnetization is zero until A reaches some critical value at which the magnetization jumps discontinuously to some finite value.

Since it has not been possible to do the detailed calculation of the A-versus-$\tilde{a}$ curve at $T=0$ in the TSCA, we determine the nature of the magnetic transi-

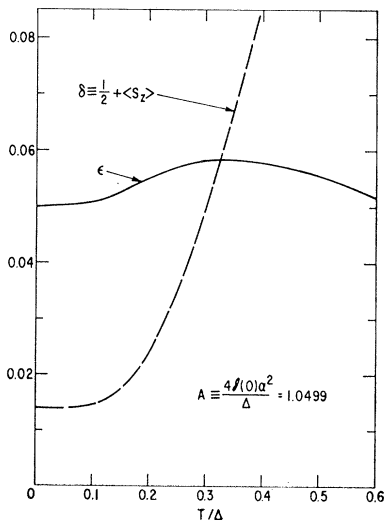

FIG. 12. Thermal variation of the correlation functions ϵ and $\delta \equiv \frac{1}{2}+\langle S_z\rangle$ which determine the susceptibility and specific-heat behavior in the TSCA. Calculations shown are for $A \equiv 4\mathcal{J}(0)\alpha^2/\Delta = 1.0499$.

tion at $T=0$ as A increases by examining the behavior of the derivative $dA/d\tilde{a}$ at $\tilde{a}=1$. If $dA/d\tilde{a}|_{\tilde{a}=1}$ is positive, this indicates that the A-versus-$\tilde{a}$ curve has gone through a minimum at some intermediate value of $\tilde{a}$, and the transition is first order. On the other hand, if $dA/d\tilde{a}|_{\tilde{a}=1}$ is negative, there is no intermediate minimum, and the transition is second order. From (6.12)

$$\frac{1}{A}\frac{dA}{d\tilde{a}}=\frac{1}{\langle S_z\rangle}\frac{d\langle S_z\rangle}{d\tilde{a}}-\frac{2}{(1-2\epsilon)}\frac{d\epsilon}{d\tilde{a}}+\frac{1}{\tilde{a}}. \quad (6.20)$$

By directly evaluating the derivatives on the right-hand side of (6.20) for $\tilde{a}=1$ at $T=0$ in the TSCA for the simple cubic lattice with nearest-neighbor exchange, and using the numerical values at $\tilde{a}=1$ and $T=0$,

$$\text{TSCA for } \tilde{a}=1,\ T=0,\quad \begin{aligned}\epsilon&=0.061,\\ \tilde{\epsilon}&=-0.046,\\ \langle S_z\rangle&=-0.4805,\end{aligned} \quad (6.21)$$

we find that $dA/d\tilde{a}=0.38A$ at $\tilde{a}=1$ and $T=0$. Since $dA/d\tilde{a}|_{\tilde{a}=1}>0$, the magnetic ordering transition in the TSCA is first order even at $T=0$.

B. Specific Heat

As shown in Fig. 11, we have calculated the specific heat in the RPA, TSCA, and molecular-field approximation for $A=1.0499$. As already stated above, this value of A gives $T_c/\Delta=0.1$ for the RPA, while the system does not order even at $T=0$ in the TSCA. (However, see Ref. 12.)

In the paramagnetic region, the molecular-field specific heat is independent of exchange. Thus, as is well known, the curve of C_v/R versus T/Δ for the Schottky anomaly is universal. In the paramagnetic regime, the Schottky anomaly is considerably broadened in the RPA and TSCA, as would be expected because of the presence of excitation waves with considerable dispersion.

It is interesting that for most of the temperature regime where both the RPA and the TSCA give paramagnetic behavior, the specific heat for the two approximations differ little. This is in contrast to the behavior of the susceptibility for the same range of temperature as that shown in Fig. 11. (See Fig. 1.) This can be understood by considering the behavior of the correlation functions ϵ and $\delta=\frac{1}{2}+\langle S_z\rangle$ shown in Fig. 12. The difference in susceptibility between the TSCA and RPA depends on ϵ being appreciable compared to δ. This is true throughout the temperature regime shown. On the other hand, the difference between the specific heats depends on $d\epsilon/dT$ being appreciable compared to $d\delta/dT$. This is true only for a narrow range of temperature at the lower-temperature part of Fig. 12. The fact that the specific heat for T/Δ just greater than 0.1 is significantly greater for the RPA can be understood by considering the excitation behavior shown in Fig. 13.

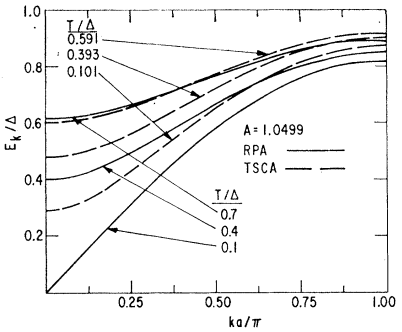

FIG. 13. Comparison of thermal variation of elementary excitation spectrum in RPA and TSCA for $A\equiv 4\mathcal{J}(0)\alpha^2/\Delta=1.0499$.

It is just in this temperature range that the RPA excitation spectrum falls sharply.

It is a matter of considerable practical importance, that while the Schottky anomaly is considerably broadened for the RPA and TSCA, even in the case where the exchange is quite substantial, the actual location of the peak is not much shifted from that for no exchange. Thus, even in the presence of large exchange, experimental location of the Schottky anomaly should give the crystal-field splitting. (Of course, when exchange is so large that the ordering temperature is comparable to the temperature of the Schottky anomaly, this simplicity vanishes. However, for rare-earth compounds, dilution of the rare earth by yttrium[4] may still allow use of the Schottky anomaly to find the crystal-field splitting.)

The specific-heat anomaly at $T_c/\Delta=0.1$ for the RPA is extremely sharp. This reflects the fact that we are at the threshold of the regime where the transition becomes first order. The presence of the two specific-heat peaks in the systems which order suggest some intriguing experiments discussed below.

C. Experimental Possibilities

While we cannot at present provide a compound that shows the properties of our model system, we can make some suggestions that may help in finding such a compound. To obtain a situation where the lowest crystal-field states of the rare earth are two singlets, we want a rare earth with integral J (Pr^{3+}, Tb^{3+}, Ho^{3+}, or Tm^{3+}) situated in a crystal field of rather low symmetry, say hexagonal. For example, Pr^{3+} in PrF_3 satisfies this criterion,[15,16] and the crystal-field splitting between the two levels is of a reasonable size (about 80–85°K).[17] On the other hand, to find substantial exchange effects of the sort we have discussed in a reasonable temperature

[15] E. Y. Wong, O. M. Stafsudd, and D. R. Johnston, J. Chem. Phys. **39**, 786 (1963).

[16] S. Kern and P. M. Raccah, J. Phys. Chem. Solids **26**, 1625 (1965).

[17] The lower of these numbers comes directly from the fluorescence measurements of Ref. 14, while the higher number comes from analysis [B. R. Cooper, 1966 (unpublished)] of the susceptibility data of Ref. 15.

range requires a rather large exchange for a rare-earth system. This suggests finding an intermetallic compound rather than an insulator.

Cubic intermetallic compounds with singlet ground states, especially the rare-earth group V compounds, are available. Indeed, the transition from Van Vleck paramagnetism to antiferromagnetism with increasing exchange (i.e., Tb content) has been observed[18] for $Tb_xY_{1-x}Sb$. However, much of the behavior becomes more complex (particularly the question of a first-order magnetic transition) when the excited state is a triplet.

[18] B. R. Cooper and O. Vogt (unpublished). Some of the results for $Tb_xY_{1-x}Sb$ are quoted in B. R. Cooper, J. Appl. Phys. **40**, 1344 (1969).

It would be very interesting, whether in a singlet-singlet or a singlet-triplet system, to study the specific heat in a number of compounds where the ratio of ordering temperature to crystal-field splitting varied. This would change the relative location and integrated area under the peaks, such as shown in Fig. 11. If alloying did not broaden out the peak at the ordering temperature too greatly, use of an alloy system such as $Tb_xY_{1-x}Sb$ to study such effects could be quite interesting.

ACKNOWLEDGMENTS

We have enjoyed interesting discussions with Professor W. Wolf. We are grateful to Miss E. Kreiger for aid with the numerical calculations.

PHYSICAL REVIEW VOLUME 185, NUMBER 2 10 SEPTEMBER 1969

Antiferromagnetic Phase Diagram and Magnetic Band Gap Shift of $NaCrS_2$

K. W. BLAZEY AND H. ROHRER
IBM Zurich Research Laboratory, 8803 Rüschlikon-ZH, Switzerland
(Received 27 March 1969)

The magnetization and differential susceptibility of the layer-structured compound $NaCrS_2$ have been measured parallel and perpendicular to the c axis in pulsed magnetic fields up to 200 kOe as a function of temperature. Antiferromagnetic ordering was observed below 18°K. For fields applied parallel to the Cr layers, a spin-flop-type transition was observed at 20 kOe and a transition to the paramagnetic phase observed at higher fields. The temperature dependence of the latter transition is found to vary as the sublattice magnetization computed from the parallel susceptibility. The in-plane and out-of-plane anisotropies are due to intraplane dipolar interactions and are of comparable magnitude, ~3 kOe. The optical absorption spectrum has been measured in the range 1–2.4 eV where the charge-transfer band gap occurs. Measurements as a function of temperature show that the *d-d* crystal-field transitions observed between 1.5 and 1.9 eV, are only slightly affected on passing through the Néel temperature, whereas the band gap shows an anomalously large blue-shift. This is thought to be evidence against the recent theory that these magnetic shifts are due to deformation potentials and magnetoelastic coupling. An alternative explanation is presented in which the band gap shift is due to the different exchange interactions in the ground and excited states.

INTRODUCTION

THE magnetic phase diagram of antiferromagnetic materials has been the subject of careful study recently, both theoretically[1,2] and experimentally. Most of the experimental studies have been restricted to the antiferromagnetic spin-flop phase transition[3] and only for materials with low Néel temperatures, such as $MnCl_2 \cdot 4\ H_2O$ [4] and $GdAlO_3$,[5] has the complete phase diagram been determined.

[1] J. Feder and E. Pytte, Phys. Rev. **168**, 640 (1968).
[2] C. J. Gorter and T. van Peski-Tinbergen, Physica **22**, 273 (1956); F. B. Anderson and H. B. Callen, Phys. Rev. **136**, 1068 (1964); H. Rohrer and H. Thomas, J. Appl. Phys. **40**, 1025 (1969).
[3] J. H. Danicar and P. R. Elliston, Phys. Letters **25A**, 720 (1967).
[4] J. E. Rives, Phys. Rev. **162**, 491 (1967).
[5] K. W. Blazey and H. Rohrer, Phys. Rev. **173**, 574 (1968); K. W. Blazey, H. Rohrer, and R. Webster, Conference on High Magnetic Fields and Their Application, University of Nottingham, England, 1969 (unpublished).

The temperature variation of the band gap of magnetic semiconductors has also been given considerable attention. The two groups of materials which have been most extensively studied are the europium chalcogenides[6] and the chromium-containing spinels.[7] On cooling these different crystals below their ordering temperatures, both red- and blue-shifts of the optical band gap have been observed. This magnetic shift in the europium chalcogenides has been ascribed to an exchange splitting of the excited state[8] and has also been related to the sample magnetization.[9] More re-

[6] G. Busch, P. Junod, and P. Wachter, Phys. Letters **12**, 822 (1965); B. E. Argyle, J. C. Suits, and M. J. Freiser, Phys. Rev. Letters **15**, 822 (1965).
[7] G. Harbeke and H. Pinch, Phys. Rev. Letters **17**, 1090 (1966).
[8] F. Rys, J. S. Helman, and W. Baltensperger, Physik Kondensierten Materie **6**, 105 (1967).
[9] G. Busch and P. Wachter, Physik Kondensierten Materie **5**, 232 (1966).